7.2 CLOUD AND PRECIPITATION PROCESSES OBSERVED IN THE 13-14 DECEMBER 2001 STORM STUDIED OVER THE OREGON CASCADES IN IMPROVE

Christopher P. Woods, Mark T. Stoelinga, John D. Locatelli, Peter V. Hobbs*
University of Washington, Seattle, WA

1. INTRODUCTION

The orographic field phase of the University of Washington's (UW) IMPROVE Project focused on the acquisition of comprehensive measurements of meteorological state parameters, polarization Doppler radar measurements, and cloud microphysical parameters to improve understanding of orographically-influenced precipitation. The Oregon Cascades, a north-south mountain barrier in west-central Oregon, is the main the topographical feature that modifies cloud processes and precipitation in this region of the Pacific Northwest. Results from an earlier study in the Washington Cascades (Hobbs et al. 1975), as well as orographic studies in other locations (Sassen et al. 1990, Demoz et al. 1993), revealed the complexity of storm systems modified by terrain. Through the use of a new generation of in-situ and remote sensing instruments in IMPROVE, we hope to add to the knowledge gained in these earlier studies and thereby improve the representations of cloud and precipitation processes in mesoscale models.

In this paper we summarize data collected during the passage of a strong occluding system over the Oregon Cascades on 13-14 December 2001. We use detailed airborne, in-situ observations to determine the primary microphysical processes influencing precipitation. We focus on differentiating between the influences of baroclinic and orographic lifting to the overall precipitation production over the mountains by considering data in reference frames relative to an upper-level baroclinic zone and to the underlying topography.

2. DATA

The north-south oriented Oregon Cascade Mountains are located about 150 km east of the Pacific Coast (Fig. 1). The NCAR S-Band dual-polarized (S-Pol) radar, which was located about 80 km west of the Cascade ridge, provided coverage across the study area including both the Willamette Valley to the west and the Cascades to the east. This radar was used for long-range weather surveillance, directing aircraft into precipitation features, and for the measurement of reflectivity, polarimetric, and air motions in precipitation features that developed in the study area.

Two aircraft were used in the field study: the NOAA P-3, which provided airborne doppler radar coverage, and the UW's Convair-580 for collecting in-situ cloud microphysical data. The Convair-580 performed a flight pattern consisting of vertically stacked horizontal legs that closely paralleled the cross-barrier flow in order to produce vertical cross-sections of microphysical information.

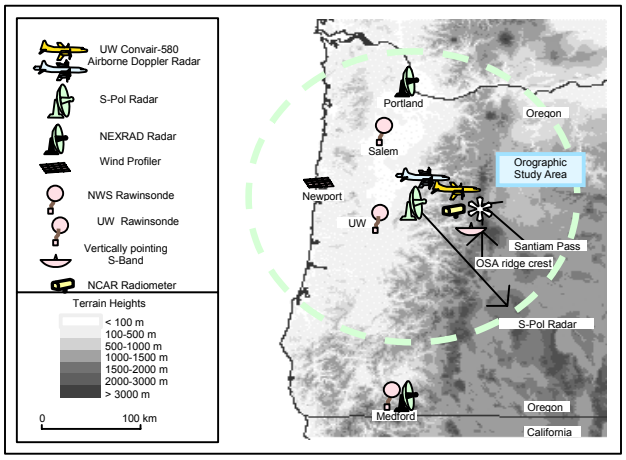

Figure 1. Study area and instrumentation

Special rawinsondes launched from Salem, Oregon, by the National Weather Service, and those from a UW mobile station sonde launch site near Creswell, Oregon, were utilized to deduce the vertical structure of the storm system. Other instrumentation and observational assets included: a snow crystal observational site along the Cascade crest, a series of raingauges extending west-east across the study area, a vertically pointing S-Band radar, and a scanning microwave radiometer for measuring column integrated liquid water on the windward side of the barrier.

3. SYNOPTIC DESCRIPTION

An occluding frontal system approached the Pacific Northwest on 13-14 December 2001, as indicated by the strengthening of the 500 hPa trough situated near Vancouver Island at 0000 UTC 14 December. Satellite imagery shows a broad cloud shield associated with this system, extending from the Pacific Coast to western Montana, which was associated with a 981 hPa surface low-pressure center (Fig. 2).

There was an upper-level, strong baroclinically-forced rainband ahead of the surface frontal rainband as it progressed across the study area. Cross-barrier flow (25-30 m s^{-1} at the 850 hPA level) was present throughout the region, which provided strong orographic forcing.

To better understand the overall structure of this storm, a time-height cross-section of rawinsonde data is shown in Fig. 3. Radar data indicated that a broad rainband, oriented in a southwest-northeast direction, moving at 13.3 m s^{-1} extended ahead of the surface front. This

*Corresponding author address: Peter V. Hobbs, Univ. of Washington, Atmos. Sciences Dept., Seattle, WA 98195-1640; email: phobbs@atmos.washington.edu

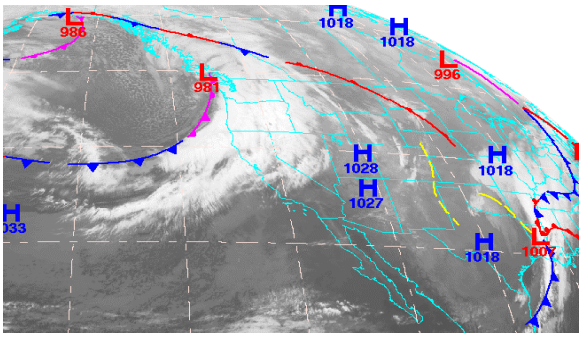

Figure 2. Satellite imagery and NCEP frontal analysis for 0000 UTC 14 December 2001

rainband played a significant role in producing precipitation over the Cascades from approximately 2200 UTC 13 December until 0200 UTC 14 December. Since the rainband was associated with an upper-level baroclinic zone, the cross-section in Fig. 3 has been assembled so that it is quasi-perpendicular to this rainband. This aids in separating influences resulting from the upper-level baroclinic forcing, and those of orographic forcing on precipitation over the mountains.

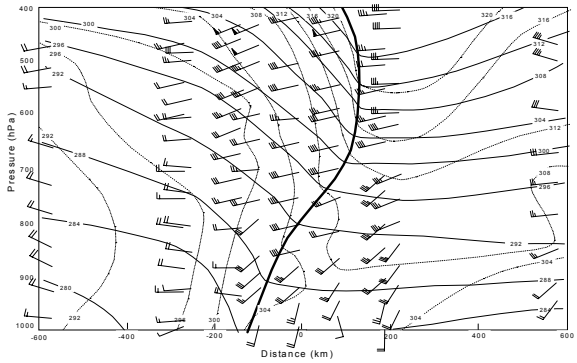

Figure 3. Time-height cross-section based on sondes launched from Salem, Oregon and UW site near Creswell, Oregon. Contours show potential temperature (solid line), equivalent potential temperature (dotted line) and wind speed (m s^{-1}). Sonde launch locations correspond to vertical wind readings.

The cross-section in Fig. 3 shows the tipped-forward orientation of the surface front as it extends upward to an upper-level baroclinic feature above 600 hPa. Equivalent potential temperature contours ahead of the frontal feature indicate the presence of a strong moisture field preceding the upper-level baroclinic region, with drier cooler air advecting into the area following its passage. Subsequent in-situ cloud microphysics data were collected aboard the Convair-580 along six horizontal legs performed immediately behind the frontal features, starting near the 470 hPa level and culminating at 800 hPa. Regions of potential instability were present between the surface and 600 hPa during the time period following the passage of the nose of the upper-level front and continued into the post-frontal period. This instability contributed to the formation of convective precipitation. Using the band-relative frame of reference shown in Fig. 3, we can now describe the cloud structures associated with the different time periods, and relate the influences of baroclinic and orographic effects on the microphysical processes important for precipitation production across the study area.

4. CLOUD STRUCTURES

Evolving cloud structures occurred throughout the passage of the occluding system. Flight transcripts from the Convair-580 during this time period, along with radar coverage, showed that three main cloud components were present in this case study: a broad altostratus cloud shield associated with the upper-level, baroclinically-forced precipitation band; a low-level stratocumulus orographic cloud, produced by the strong flow across the mountains; and non-orographic convective clouds that formed in the intra-frontal region between the passage of the upper-level band and the surface front, and in the post-frontal conditions.

The altostratus cloud deck that accompanied the upper-level baroclinic forcing was deep and diffuse in nature. However, the layering that was often observed in frontal clouds over the Washington Cascades (Hobbs et al. 1975) was not apparent in this case. The altostratus cloud had tops around 8-9 km and extended down to about 4 km. While this cloud lacked high liquid water contents, the existence of occasional embedded droplet clouds indicated a relatively high level of saturation throughout the altostratus cloud along the Convair-580 flight legs between 6 km and 4 km.

At lower levels, the primary cloud structure was orographically influenced, as strong upslope flow resulted in the formation of stratocumulus clouds above the barrier. The stratocumulus extended up to the base of the altostratus cloud shield as it passed through the study area. The top of the orographic stratocumulus cloud was capped near the 4 km level by the advection of cold dry air behind the migratory upper-level cloud shield. In-flight scientists reported small-scale turrets within the orographic cloud; these turrets produced pockets of increased cloud liquid water. The presence of this liquid-water rich orographic cloud played a significant role in the production of precipitation throughout this case study, and will be considered in subsequent sections.

Convective clouds, with tops near 4 km, dominated the time period after the passage of the upper-level cloud shield and prior to the passage of the surface frontal rainband. Shallower convection was present in the post-frontal regime, as tops subsided to 2-3 km.

5. MICROPHYSICAL PARAMETERS AND PROCESSES

a. Cloud Liquid Water

Previous studies have shown that cloud liquid water (CLW) plays a significant role in the growth of precipitation within wintertime orographically-influenced storm systems (e.g., Hobbs et al. 1975, Sassen et al. 1990, Demoz et al. 1993). Cloud liquid water is also important because it can be compared directly to model simulations. For the 13-14 December 2001 case study we used two sources for CLW measurements: in-situ data collected

from the Convair-580 and ground-based microwave radiometer measurements of vertically-integrated CLW. After presenting the time evolution of CLW and considering the regions of enhanced CLW recorded in flight, our discussion will focus on the influences of CLW on precipitation character and growth.

In-situ measurements of CLW, measured by the PVM-100A optical sensor on the Convair-580, show relatively low values in the upper-level cloud band, ranging from 0.0-0.05 g m^{-3} (flight legs between numbers 1-8 in Fig. 4). On descending into the stratocumulus orographic cloud (flight leg connecting 8 and 9), increased CLW was encountered, with a peak around 0.4 g m^{-3} in an embedded turret within the orographic cloud. The remaining flight legs indicated a significant influence of orography on CLW, with the largest enhancement occurring above the windward Cascade slopes. Suppression of CLW occurred in the lee of the mountains, where measured values decreased dramatically to nearly 0.0 g m^{-3}. Ice crystal analyses, presented later in this paper, show the influence of these different liquid water regimes on the nature of the ice crystals observed along the flight tracks.

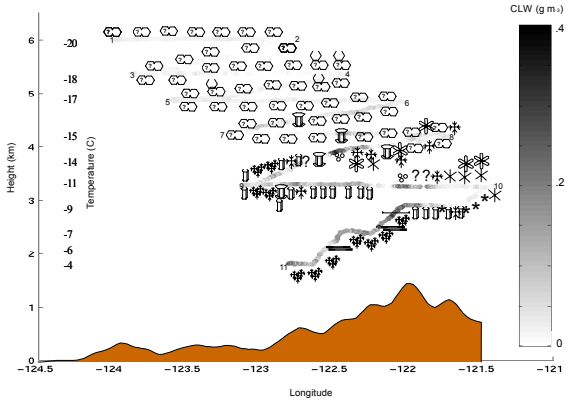

Figure 4. Cloud liquid water (CLW) from in-situ measurements aboard the Convair-580 (g m^{-3}) plotted in grayscale along the various aircraft flight legs (numbered 1 through 11). Crystal types are shown along the legs, with crystal habits in this and other figures classified according to the scheme proposed by Magono and Lee (1966), with symbol descriptions given in Fig. 6b.

The NCAR microwave radiometer (deployed just upstream of the Cascade crest, at an elevation of 1138 m) provided measurements of vertically-integrated CLW (expressed as liquid water depth) throughout the passage of the 13-14 December 2001 storm. As frontal features passed over the radiometer site, fluctuations are seen in the integrated CLW throughout the time period of interest (Fig. 5). Assuming a Marshall-Palmer distribution of droplets (Marshall and Palmer 1948) within the rainlayer, the depth of LW (cm) from this layer was calculated by determining its depth and rainrate, and subtracting this value from the integrated radiometer measurement to derive the CLW shown in Fig. 5. The freezing level was determined by locating the melting level, as indicated by a bright band measured by a nearby vertically pointing S-Band radar, and the rainrate within the rain layer as measured by a co-located raingauge. As can be seen in Fig. 5, significant amounts of CLW existed throughout the storm. Maximum CLW depths near 0.18 cm were present in the pre-frontal conditions, as strong southwesterly flow across the mountains provided the necessary lifting to enhance CLW production along the western slopes of the Cascades. Precipitating ice particles in pre-frontal showers (with tops near 4.5 km) depleted CLW through riming. During the passage of the upper-level baroclinic rainband, CLW depth ranged from 0.05 cm to 0.12 cm, with the maximum value occurring along the back edge of the upper-level altostratus cloud shield as the fallout of ice particles diminished following the passage of the upper band. This regime was followed by convective precipitation ahead of the surface frontal passage. The CLW measurements during this period, while diminished, exhibit a spiky behavior due to intermittent convective showers that depleted CLW. The CLW depth fell to nearly 0.0 cm at the leading edge of the surface frontal passage. This suggests that either cloud water was not present at this time, or that any precipitation falling during this time period very efficiently scavenged what CLW was present. The latter seems more likely, since crystal observations made on the ground during this time period reveal predominantly heavily rimed crystals and graupel (see next section).

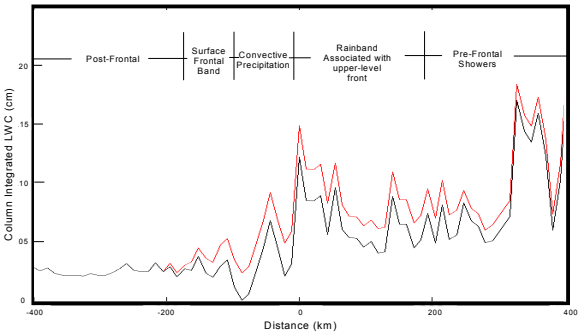

Figure 5. Vertically integrated liquid water from the NCAR radiometer projected onto time-height coordinates from the cross-section in Fig. 3. Sum of rain and cloud water (red line), and cloud water only (black line).

b. *Ice Crystal Analysis*

This section focuses on ground-based ice crystal observations made along the Cascade crest, and in-situ ice crystal data obtained aboard the Convair-580 aircraft. Through use of an OAP 2D-C diode-imaging probe mounted on Convair-580, we deduced crystal habits at various altitudes and temperatures within the storm. This information, together with the observations along the Cascade crest, show that the primary mechanisms affecting precipitation growth, were growth of ice particles by vapor diffusion at all levels, and growth by riming below 4 km. Aggregates were also present below 4 km during the storm passage. We will consider the airborne in-situ crystal data with respect to the upper-level baroclinic band previously discussed, and relative to the underlying terrain. The ground-based observations will be projected

onto the cross-sectional frame of reference described previously, since they were made at a fixed point along the Cascade crest.

The dominant crystal habits along the Convair flight track, in a reference frame relative to the upper-level precipitation band, show how the crystal type changed in relation to synoptic features (Fig. 6). Due to the motion of the band (nearly 20.5 m s^{-1} in the direction of the west-east cross-sectional view), the stacked legs of the Convair-580 took on a tipped-forward orientation. The four uppermost flight legs were in the upper altostratus shield associated with the upper-level baroclinic region. The 2-D particle images collected along these legs show primarily cold-type crystals, such as assemblages of sectors, sideplanes, and plates. Also present were occasional unrimed individual plates. These crystal habits indicate that crystal growth occurred via vapor diffusion. Evidence of rimed particles was not seen until lower flight legs within the orographic lifting zone in regions of higher CLW production. Below the upper-level altostratus deck, several different crystal habits were present in the orographic cloud, the two primary types were dendrites and their aggregates and columnar-shaped crystals. The dendritic crystal formation indicates water supersaturation up to 4 km. Moderately to extensively rimed crystals, which contributed significantly to the overall precipitation budget, were present along the lower flight legs (below 4 km).

Regions of active crystal production, and those lacking active production, can be identified through both the sizes and shapes of crystals and in-situ temperatures. One region of column formation was at the 3.6 km level, where high concentrations of uniformly sized columns, 300-400 μm in length, were present in the absence of other crystal types (Fig 6a, A1). These columnar crystals grew in length before being encountered at the 3.3 km level (Fig. 6a, A2). At 2.5 km, aggregates of dendrites were encountered (Fig. 6a, B), showing that precipitation growth by aggregation was occurring here, but there was no active production of new crystals. With an ambient temperature of –6 °C at this locale, we would expect new crystal production in the form of needles and/or sheaths, rather than aggregates of dendrites that form near –15 °C.

The microphysical processes responsible for influencing precipitation formation and growth, deduced from the in-situ crystal data in a band-relative sense, must also be considered in a terrain-relative reference frame to better understand the role of topography in precipitation production. Significant orographic influences were apparent along those flight legs closest in altitude to the terrain (Fig. 4). In the lower flight legs within the orographic lifting zone, 2-D particle images showed dendritic development, indicating water supersaturated conditions, as well as growth at water subsaturation (columns). There were rapid changes in supersaturation and crystal type; in some locations, these changes occurred over a distance of 1 km or less, possibly due to local changes in terrain and updraft velocity. Topographical influences also produced increases in CLW over the windward slopes of the Cascade ridges,

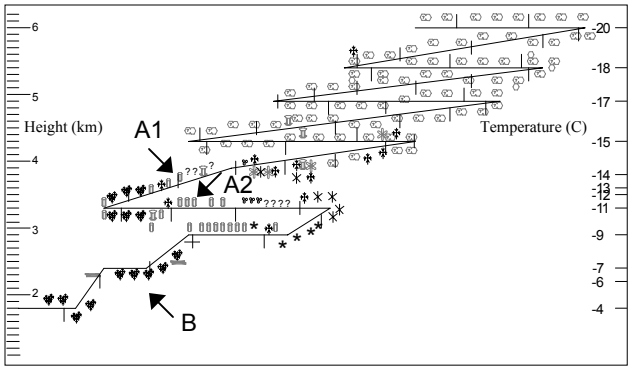

Figure 6 *(a.) Convair-580 flight track relative to the upper-level baroclinic rainband. In-situ crystal identification between 2318 UTC 13-December 2001 to 0308 UTC 14-December 2001. (b.) Key to crystal types.*

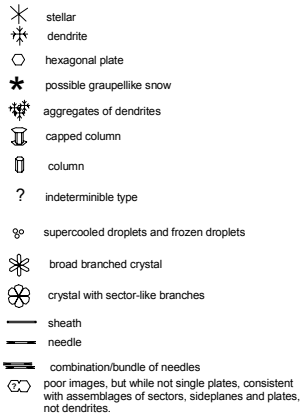

6b.) Key to dominant crystal types shown in Fig. 6a and Fig. 4

leading to increased riming of crystals.

Ground-based observations showed that crystal shapes and character were generally lost by the time the crystals reached the ground. Graupel and graupellike snow were observed throughout the observational period (2330–0730 UTC 13-14 December). Dendritic and broad-branched crystals were observed occasionally beneath a layer of heavy riming. These observations show the importance of growth by riming, particularly below 2-3 km.

6. SUMMARY

The 13-14 December 2001 storm that passed over the Oregon Cascades involved baroclinically-forced and topographically-forced influences on precipitation strength and character. The ice crystal growth processes found in this case are summarized in Fig. 7. Crystal growth by vapor diffusion occurred throughout the upper levels of the storm and within the lower-level orographic cloud between 2-4 km. Crystal growth due to riming was confined to the region of increased CLW located in the orographic lifting zone below 4 km. Riming was a significant contributor to precipitation growth, as indicated by the ice particles observed near the Cascade crest that included: heavily rimed crystals, graupel, and graupel-like

snow. The presence of aggregates was limited to dendrites within the orographic cloud.

We are currently determining the quantitative contributions to the overall rainrate of precipitation generated in the upper-level baroclinically forced rainband and the lower-level orographic cloud. These calculations will be utilized to compare with an MM5 model run of this case (e.g., Garvert et al. 2003), with the goal of locating deficiencies in, and improving as necessary, the parameterizations of cloud and precipitation processes in such models.

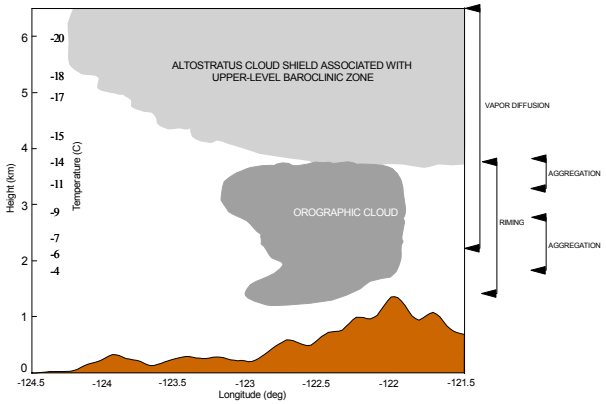

Figure 7. Summary of precipitation growth mechanisms observed over the Oregon Cascades in the 13-14 December 2001 orographic precipitation case study. The levels at which various growth mechanism occurred are indicated.

7. ACKNOWLEDGMENTS

Research supported by grant ATM-9632580 from the Mesoscale Dynamic Meteorology Program, Atmospheric Sciences Division, NSF.

8. REFERENCES

Demoz, B.B., R. Zhang, and R.L. Pitter, 1993: An Analysis of Sierra Nevada Winter Orographic Storms: Ground-based Ice-Crystal Observations. *J. Appl. Meteor.*, **32**, 1826-1836.

Garvert, M., C. Mass, and B. Colle, 2003: Modeling of the 13-14 December 2001 IMPROVE 2 Case. 10th Mesoscale Conference Extended Manuscript

Hobbs, P.V., R.A. Houze, and T.J. Matejka, 1975: The Dynamical and Microphysical Structure of an Occluded Frontal System and its Modification by Orography. *J. Atmos. Sci.*, **32**, 1542-1562.

Magono, C. and C.W. Lee, 1966: Meteorological Classification of Natural Snow Crystals. *J. Faculty Sci.*, **II**, 321-335.

Marshall, J.S., and W. M. Palmer, 1948: The Distribution of Raindrops with Size. *J. Atmos. Sci.,* **5**, 165-166.

Sassen et. al., 1990: Investigations of a Winter Mountain Storm in Utah. Part II: Mesoscale Structure, Supercooled Liquid Water Development, and Precipitation Processes. *J. Atmos. Sci.*, **47**, 1323-1349.